

**Measurements of the branching fractions and CP asymmetries of $B^\pm \rightarrow J/\psi \pi^\pm$
and $B^\pm \rightarrow \psi(2S) \pi^\pm$ decays**

- R. Aaij,³⁸ C. Abellan Beteta,^{33,n} B. Adeva,³⁴ M. Adinolfi,⁴³ C. Adrover,⁶ A. Affolder,⁴⁹ Z. Ajaltouni,⁵ J. Albrecht,³⁵ F. Alessio,³⁵ M. Alexander,⁴⁸ S. Ali,³⁸ G. Alkhazov,²⁷ P. Alvarez Cartelle,³⁴ A. A. Alves, Jr.,²² S. Amato,² Y. Amhis,³⁶ J. Anderson,³⁷ R. B. Appleby,⁵¹ O. Aquines Gutierrez,¹⁰ F. Archilli,^{18,35} A. Artamonov,³² M. Artuso,^{53,35} E. Aslanides,⁶ G. Auriemma,^{22,m} S. Bachmann,¹¹ J. J. Back,⁴⁵ V. Balagura,^{28,35} W. Baldini,¹⁶ R. J. Barlow,⁵¹ C. Barschel,³⁵ S. Barsuk,⁷ W. Barter,⁴⁴ A. Bates,⁴⁸ C. Bauer,¹⁰ Th. Bauer,³⁸ A. Bay,³⁶ I. Bediaga,¹ S. Belogurov,²⁸ K. Belous,³² I. Belyaev,²⁸ E. Ben-Haim,⁸ M. Benayoun,⁸ G. Bencivenni,¹⁸ S. Benson,⁴⁷ J. Benton,⁴³ R. Bernet,³⁷ M.-O. Bettler,¹⁷ M. van Beuzekom,³⁸ A. Bien,¹¹ S. Bifani,¹² T. Bird,⁵¹ A. Bizzeti,^{17,h} P. M. Bjørnstad,⁵¹ T. Blake,³⁵ F. Blanc,³⁶ C. Blanks,⁵⁰ J. Blouw,¹¹ S. Blusk,⁵³ A. Bobrov,³¹ V. Bocci,²² A. Bondar,³¹ N. Bondar,²⁷ W. Bonivento,¹⁵ S. Borghi,^{48,51} A. Borgia,⁵³ T. J. V. Bowcock,⁴⁹ C. Bozzi,¹⁶ T. Brambach,⁹ J. van den Brand,³⁹ J. Bressieux,³⁶ D. Brett,⁵¹ M. Britsch,¹⁰ T. Britton,⁵³ N. H. Brook,⁴³ H. Brown,⁴⁹ A. Büchler-Germann,³⁷ I. Burducea,²⁶ A. Bursche,³⁷ J. Buytaert,³⁵ S. Cadeddu,¹⁵ O. Callot,⁷ M. Calvi,^{20,j} M. Calvo Gomez,^{33,n} A. Camboni,³³ P. Campana,^{18,35} A. Carbone,¹⁴ G. Carboni,^{21,k} R. Cardinale,^{19,35,i} A. Cardini,¹⁵ L. Carson,⁵⁰ K. Carvalho Akiba,² G. Casse,⁴⁹ M. Cattaneo,³⁵ Ch. Cauet,⁹ M. Charles,⁵² Ph. Charpentier,³⁵ N. Chiapolini,³⁷ K. Ciba,³⁵ X. Cid Vidal,³⁴ G. Ciezarek,⁵⁰ P. E. L. L. Clarke,^{47,35} M. Clemencic,³⁵ H. V. Cliff,⁴⁴ J. Closier,³⁵ C. Coca,²⁶ V. Coco,³⁸ J. Cogan,⁶ P. Collins,³⁵ A. Comerma-Montells,³³ A. Contu,⁵² A. Cook,⁴³ M. Coombes,⁴³ G. Corti,³⁵ B. Couturier,³⁵ G. A. Cowan,³⁶ R. Currie,⁴⁷ C. D'Ambrosio,³⁵ P. David,⁸ P. N. Y. David,³⁸ I. De Bonis,⁴ K. de Bruyn,³⁸ S. De Capua,^{21,k} M. De Cian,³⁷ J. M. De Miranda,¹ L. De Paula,² P. De Simone,¹⁸ D. Decamp,⁴ M. Deckenhoff,⁹ H. Degaudenzi,^{36,35} L. Del Buono,⁸ C. Deplano,¹⁵ D. Derkach,^{14,35} O. Deschamps,⁵ F. Dettori,³⁹ J. Dickens,⁴⁴ H. Dijkstra,³⁵ P. Diniz Batista,¹ F. Domingo Bonal,^{33,n} S. Donleavy,⁴⁹ F. Dordei,¹¹ A. Dosil Suárez,³⁴ D. Dossett,⁴⁵ A. Dovbnya,⁴⁰ F. Dupertuis,³⁶ R. Dzhelyadin,³² A. Dziurda,²³ S. Easo,⁴⁶ U. Egede,⁵⁰ V. Egorychev,²⁸ S. Eidelman,³¹ D. van Eijk,³⁸ F. Eisele,¹¹ S. Eisenhardt,⁴⁷ R. Ekelhof,⁹ L. Eklund,⁴⁸ Ch. Elsasser,³⁷ D. Elsby,⁴² D. Esperante Pereira,³⁴ A. Falabella,^{16,14,e} C. Färber,¹¹ G. Fardell,⁴⁷ C. Farinelli,³⁸ S. Farry,¹² V. Fave,³⁶ V. Fernandez Albor,³⁴ M. Ferro-Luzzi,³⁵ S. Filippov,³⁰ C. Fitzpatrick,⁴⁷ M. Fontana,¹⁰ F. Fontanelli,^{19,i} R. Forty,³⁵ O. Francisco,² M. Frank,³⁵ C. Frei,³⁵ M. Frosini,^{17,f} S. Furcas,²⁰ A. Gallas Torreira,³⁴ D. Galli,^{14,c} M. Gandelman,² P. Gandini,⁵² Y. Gao,³ J.-C. Garnier,³⁵ J. Garofoli,⁵³ J. Garra Tico,⁴⁴ L. Garrido,³³ D. Gascon,³³ C. Gaspar,³⁵ R. Gauld,⁵² N. Gauvin,³⁶ M. Gersabeck,³⁵ T. Gershon,^{45,35} Ph. Ghez,⁴ V. Gibson,⁴⁴ V. V. Gligorov,³⁵ C. Göbel,⁵⁴ D. Golubkov,²⁸ A. Golutvin,^{50,28,35} A. Gomes,² H. Gordon,⁵² M. Grabalosa Gándara,³³ R. Graciani Diaz,³³ L. A. Granado Cardoso,³⁵ E. Graugés,³³ G. Graziani,¹⁷ A. Grecu,²⁶ E. Greening,⁵² S. Gregson,⁴⁴ B. Gui,⁵³ E. Gushchin,³⁰ Yu. Guz,³² T. Gys,³⁵ C. Hadjivassiliou,⁵³ G. Haefeli,³⁶ C. Haen,³⁵ S. C. Haines,⁴⁴ T. Hampson,⁴³ S. Hansmann-Menzemer,¹¹ R. Harji,⁵⁰ N. Harnew,⁵² J. Harrison,⁵¹ P. F. Harrison,⁴⁵ T. Hartmann,⁵⁵ J. He,⁷ V. Heijne,³⁸ K. Hennessy,⁴⁹ P. Henrard,⁵ J. A. Hernando Morata,³⁴ E. van Herwijnen,³⁵ E. Hicks,⁴⁹ K. Holubyev,¹¹ P. Hopchev,⁴ W. Hulsbergen,³⁸ P. Hunt,⁵² T. Huse,⁴⁹ R. S. Huston,¹² D. Hutchcroft,⁴⁹ D. Hynds,⁴⁸ V. Iakovenko,⁴¹ P. Ilten,¹² J. Imong,⁴³ R. Jacobsson,³⁵ A. Jaeger,¹¹ M. Jahjah Hussein,⁵ E. Jans,³⁸ F. Jansen,³⁸ P. Jaton,³⁶ B. Jean-Marie,⁷ F. Jing,³ M. John,⁵² D. Johnson,⁵² C. R. Jones,⁴⁴ B. Jost,³⁵ M. Kaballo,⁹ S. Kandybei,⁴⁰ M. Karacson,³⁵ T. M. Karbach,⁹ J. Keaveney,¹² I. R. Kenyon,⁴² U. Kerzel,³⁵ T. Ketel,³⁹ A. Keune,³⁶ B. Khanji,⁶ Y. M. Kim,⁴⁷ M. Knecht,³⁶ R. F. Koopman,³⁹ P. Koppenburg,³⁸ M. Korolev,²⁹ A. Kozlinskiy,³⁸ L. Kravchuk,³⁰ K. Kreplin,¹¹ M. Kreps,⁴⁵ G. Krocker,¹¹ P. Krokovny,¹¹ F. Kruse,⁹ K. Kruzelecki,³⁵ M. Kucharczyk,^{20,23,35,j} V. Kudryavtsev,³¹ T. Kvaratskheliya,^{28,35} V. N. La Thi,³⁶ D. Lacarrere,³⁵ G. Lafferty,⁵¹ A. Lai,¹⁵ D. Lambert,⁴⁷ R. W. Lambert,³⁹ E. Lanciotti,³⁵ G. Lanfranchi,¹⁸ C. Langenbruch,¹¹ T. Latham,⁴⁵ C. Lazzeroni,⁴² R. Le Gac,⁶ J. van Leerdam,³⁸ J.-P. Lees,⁴ R. Lefèvre,⁵ A. Leflat,^{29,35} J. Lefrançois,⁷ O. Leroy,⁶ T. Lesiak,²³ L. Li,³ L. Li Gioi,⁵ M. Lieng,⁹ M. Liles,⁴⁹ R. Lindner,³⁵ C. Linn,¹¹ B. Liu,³ G. Liu,³⁵ J. von Loeben,²⁰ J. H. Lopes,² E. Lopez Asamar,³³ N. Lopez-March,³⁶ H. Lu,³ J. Luisier,³⁶ A. Mac Raighne,⁴⁸ F. Machefert,⁷ I. V. Machikhiliyan,^{4,28} F. Maciuc,¹⁰ O. Maev,^{27,35} J. Magnin,¹ S. Malde,⁵² R. M. D. Mamunur,³⁵ G. Manca,^{15,d} G. Mancinelli,⁶ N. Mangiafave,⁴⁴ U. Marconi,¹⁴ R. Märki,³⁶ J. Marks,¹¹ G. Martellotti,²² A. Martens,⁸ L. Martin,⁵² A. Martín Sánchez,⁷ M. Martinelli,³⁸ D. Martinez Santos,³⁵ A. Massafferri,¹ Z. Mathe,¹² C. Matteuzzi,²⁰ M. Matveev,²⁷ E. Maurice,⁶ B. Maynard,⁵³ A. Mazurov,^{16,30,35} G. McGregor,⁵¹ R. McNulty,¹² M. Meissner,¹¹ M. Merk,³⁸ J. Merkel,⁹ S. Miglioranzi,³⁵ D. A. Milanes,¹³ M.-N. Minard,⁴ J. Molina Rodriguez,⁵⁴ S. Monteil,⁵ D. Moran,¹² P. Morawski,²³ R. Mountain,⁵³ I. Mous,³⁸ F. Muheim,⁴⁷ K. Müller,³⁷ R. Muresan,²⁶ B. Muryn,²⁴ B. Muster,³⁶ J. Mylroie-Smith,⁴⁹ P. Naik,⁴³ T. Nakada,³⁶ R. Nandakumar,⁴⁶ I. Nasteva,¹ M. Needham,⁴⁷ N. Neufeld,³⁵ A. D. Nguyen,³⁶ C. Nguyen-Mau,^{36,o} M. Nicol,⁷ V. Niess,⁵ N. Nikitin,²⁹ T. Nikodem,¹¹ A. Nomerotski,^{52,35} A. Novoselov,³² A. Oblakowska-Mucha,²⁴ V. Obratzsov,³² S. Oggero,³⁸

R. AAIJ *et al.*

PHYSICAL REVIEW D 85, 091105(R) (2012)

- S. Ogilvy,⁴⁸ O. Okhrimenko,⁴¹ R. Oldeman,^{15,35,d} M. Orlandea,²⁶ J. M. Otalora Goicochea,² P. Owen,⁵⁰ B. K. Pal,⁵³
 J. Palacios,³⁷ A. Palano,^{13,b} M. Palutan,¹⁸ J. Panman,³⁵ A. Papanestis,⁴⁶ M. Pappagallo,⁴⁸ C. Parkes,⁵¹ C. J. Parkinson,⁵⁰
 G. Passaleva,¹⁷ G. D. Patel,⁴⁹ M. Patel,⁵⁰ S. K. Paterson,⁵⁰ G. N. Patrick,⁴⁶ C. Patrignani,^{19,i} C. Pavel-Nicorescu,²⁶
 A. Pazos Alvarez,³⁴ A. Pellegrino,³⁸ G. Penso,^{22,l} M. Pepe Altarelli,³⁵ S. Perazzini,^{14,c} D. L. Perego,^{20,j} E. Perez Trigo,³⁴
 A. Pérez-Calero Yzquierdo,³³ P. Perret,⁵ M. Perrin-Terrin,⁶ G. Pessina,²⁰ A. Petrolini,^{19,i} A. Phan,⁵³ E. Picatoste Olloqui,³³
 B. Pie Valls,³³ B. Pietrzyk,⁴ T. Pilar,⁴⁵ D. Pinci,²² R. Plackett,⁴⁸ S. Playfer,⁴⁷ M. Plo Casasus,³⁴ G. Polok,²³ A. Poluektov,^{45,31}
 E. Polycarpo,² D. Popov,¹⁰ B. Popovici,²⁶ C. Potterat,³³ A. Powell,⁵² J. Prisciandaro,³⁶ V. Pugatch,⁴¹ A. Puig Navarro,³³
 W. Qian,⁵³ J. H. Rademacker,⁴³ B. Rakotomiaramanana,³⁶ M. S. Rangel,² I. Raniuk,⁴⁰ G. Raven,³⁹ S. Redford,⁵²
 M. M. Reid,⁴⁵ A. C. dos Reis,¹ S. Ricciardi,⁴⁶ A. Richards,⁵⁰ K. Rinnert,⁴⁹ D. A. Roa Romero,⁵ P. Robbe,⁷ E. Rodrigues,^{48,51}
 F. Rodrigues,² P. Rodriguez Perez,³⁴ G. J. Rogers,⁴⁴ S. Roiser,³⁵ V. Romanovsky,³² M. Rosello,^{33,n} J. Rouvinet,³⁶ T. Ruf,³⁵
 H. Ruiz,³³ G. Sabatino,^{21,k} J. J. Saborido Silva,³⁴ N. Sagidova,²⁷ P. Sail,⁴⁸ B. Saitta,^{15,d} C. Salzmann,³⁷ M. Sannino,^{19,i}
 R. Santacesaria,²² C. Santamarina Rios,³⁴ R. Santinelli,³⁵ E. Santovetti,^{21,k} M. Sapunov,⁶ A. Sarti,^{18,l} C. Satriano,^{22,m}
 A. Satta,²¹ M. Savrie,^{16,e} D. Savrina,²⁸ P. Schaack,⁵⁰ M. Schiller,³⁹ H. Schindler,³⁵ S. Schleich,⁹ M. Schlupp,⁹
 M. Schmelling,¹⁰ B. Schmidt,³⁵ O. Schneider,³⁶ A. Schopper,³⁵ M.-H. Schune,⁷ R. Schwemmer,³⁵ B. Sciascia,¹⁸
 A. Sciubba,^{18,l} M. Seco,³⁴ A. Semennikov,²⁸ K. Senderowska,²⁴ I. Sepp,⁵⁰ N. Serra,³⁷ J. Serrano,⁶ P. Seyfert,¹¹ M. Shapkin,³²
 I. Shapoval,^{40,35} P. Shatalov,²⁸ Y. Shcheglov,²⁷ T. Shears,⁴⁹ L. Shekhtman,³¹ O. Shevchenko,⁴⁰ V. Shevchenko,²⁸ A. Shires,⁵⁰
 R. Silva Coutinho,⁴⁵ T. Skwarnicki,⁵³ N. A. Smith,⁴⁹ E. Smith,^{52,46} K. Sobczak,⁵ F. J. P. Soler,⁴⁸ A. Solomin,⁴³ F. Soomro,^{18,35}
 B. Souza De Paula,² B. Spaan,⁹ A. Sparkes,⁴⁷ P. Spradlin,⁴⁸ F. Stagni,³⁵ S. Stahl,¹¹ O. Steinkamp,³⁷ S. Stoica,²⁶ S. Stone,^{53,35}
 B. Storaci,³⁸ M. Straticiuc,²⁶ U. Straumann,³⁷ V. K. Subbiah,³⁵ S. Swientek,⁹ M. Szczekowski,²⁵ P. Szczypka,³⁶ T. Szumlak,²⁴
 S. T'Jampens,⁴ E. Teodorescu,²⁶ F. Teubert,³⁵ C. Thomas,⁵² E. Thomas,³⁵ J. van Tilburg,¹¹ V. Tisserand,⁴ M. Tobin,³⁷
 S. Tolk,³⁹ S. Topp-Joergensen,⁵² N. Torr,⁵² E. Tournefier,^{4,50} S. Tourneur,³⁶ M. T. Tran,³⁶ A. Tsaregorodtsev,⁶ N. Tuning,³⁸
 M. Ubeda Garcia,³⁵ A. Ukleja,²⁵ U. Uwer,¹¹ V. Vagnoni,¹⁴ G. Valenti,¹⁴ R. Vazquez Gomez,³³ P. Vazquez Regueiro,³⁴
 S. Vecchi,¹⁶ J. J. Velthuis,⁴³ M. Veltri,^{17,g} B. Viaud,⁷ I. Videau,⁷ D. Vieira,² X. Vilasis-Cardona,^{33,n} J. Visniakov,³⁴
 A. Vollhardt,³⁷ D. Volyanskyy,¹⁰ D. Voong,⁴³ A. Vorobyev,²⁷ V. Vorobyev,³¹ H. Voss,¹⁰ R. Waldi,⁵⁵ S. Wandernoth,¹¹
 J. Wang,⁵³ D. R. Ward,⁴⁴ N. K. Watson,⁴² A. D. Webber,⁵¹ D. Websdale,⁵⁰ M. Whitehead,⁴⁵ D. Wiedner,¹¹ L. Wiggers,³⁸
 G. Wilkinson,⁵² M. P. Williams,^{45,46} M. Williams,⁵⁰ F. F. Wilson,⁴⁶ J. Wishahi,⁹ M. Witek,²³ W. Witzeling,³⁵ S. A. Wotton,⁴⁴
 K. Wyllie,³⁵ Y. Xie,⁴⁷ F. Xing,⁵² Z. Xing,⁵³ Z. Yang,³ R. Young,⁴⁷ O. Yushchenko,³² M. Zangoli,¹⁴ M. Zavertyaev,^{10,a}
 F. Zhang,³ L. Zhang,⁵³ W. C. Zhang,¹² Y. Zhang,³ A. Zhelezov,¹¹ L. Zhong,³ and A. Zvyagin³⁵

(LHCb Collaboration)

¹*Centro Brasileiro de Pesquisas Físicas (CBPF), Rio de Janeiro, Brazil*²*Universidade Federal do Rio de Janeiro (UFRJ), Rio de Janeiro, Brazil*³*Center for High Energy Physics, Tsinghua University, Beijing, China*⁴*LAPP, Université de Savoie, CNRS/IN2P3, Annecy-Le-Vieux, France*⁵*Clermont Université, Université Blaise Pascal, CNRS/IN2P3, LPC, Clermont-Ferrand, France*⁶*CPPM, Aix-Marseille Université, CNRS/IN2P3, Marseille, France*⁷*LAL, Université Paris-Sud, CNRS/IN2P3, Orsay, France*⁸*LPNHE, Université Pierre et Marie Curie, Université Paris Diderot, CNRS/IN2P3, Paris, France*⁹*Fakultät Physik, Technische Universität Dortmund, Dortmund, Germany*¹⁰*Max-Planck-Institut für Kernphysik (MPIK), Heidelberg, Germany*¹¹*Physikalisch Institut, Ruprecht-Karls-Universität Heidelberg, Heidelberg, Germany*¹²*School of Physics, University College Dublin, Dublin, Ireland*¹³*Sezione INFN di Bari, Bari, Italy*¹⁴*Sezione INFN di Bologna, Bologna, Italy*¹⁵*Sezione INFN di Cagliari, Cagliari, Italy*¹⁶*Sezione INFN di Ferrara, Ferrara, Italy*¹⁷*Sezione INFN di Firenze, Firenze, Italy*¹⁸*Laboratori Nazionali dell'INFN di Frascati, Frascati, Italy*¹⁹*Sezione INFN di Genova, Genova, Italy*²⁰*Sezione INFN di Milano Bicocca, Milano, Italy*²¹*Sezione INFN di Roma Tor Vergata, Roma, Italy*²²*Sezione INFN di Roma La Sapienza, Roma, Italy*²³*Henryk Niewodniczanski Institute of Nuclear Physics Polish Academy of Sciences, Kraków, Poland*²⁴*AGH University of Science and Technology, Kraków, Poland*

²⁵Soltan Institute for Nuclear Studies, Warsaw, Poland²⁶Horia Hulubei National Institute of Physics and Nuclear Engineering, Bucharest-Magurele, Romania²⁷Petersburg Nuclear Physics Institute (PNPI), Gatchina, Russia²⁸Institute of Theoretical and Experimental Physics (ITEP), Moscow, Russia²⁹Institute of Nuclear Physics, Moscow State University (SINP MSU), Moscow, Russia³⁰Institute for Nuclear Research of the Russian Academy of Sciences (INR RAN), Moscow, Russia³¹Budker Institute of Nuclear Physics (SB RAS) and Novosibirsk State University, Novosibirsk, Russia³²Institute for High Energy Physics (IHEP), Protvino, Russia³³Universitat de Barcelona, Barcelona, Spain³⁴Universidad de Santiago de Compostela, Santiago de Compostela, Spain³⁵European Organization for Nuclear Research (CERN), Geneva, Switzerland³⁶Ecole Polytechnique Fédérale de Lausanne (EPFL), Lausanne, Switzerland³⁷Physik-Institut, Universität Zürich, Zürich, Switzerland³⁸Nikhef National Institute for Subatomic Physics, Amsterdam, The Netherlands³⁹Nikhef National Institute for Subatomic Physics and Vrije Universiteit, Amsterdam, The Netherlands⁴⁰NSC Kharkiv Institute of Physics and Technology (NSC KIPT), Kharkiv, Ukraine⁴¹Institute for Nuclear Research of the National Academy of Sciences (KINR), Kyiv, Ukraine⁴²University of Birmingham, Birmingham, United Kingdom⁴³H.H. Wills Physics Laboratory, University of Bristol, Bristol, United Kingdom⁴⁴Cavendish Laboratory, University of Cambridge, Cambridge, United Kingdom⁴⁵Department of Physics, University of Warwick, Coventry, United Kingdom⁴⁶STFC Rutherford Appleton Laboratory, Didcot, United Kingdom⁴⁷School of Physics and Astronomy, University of Edinburgh, Edinburgh, United Kingdom⁴⁸School of Physics and Astronomy, University of Glasgow, Glasgow, United Kingdom⁴⁹Oliver Lodge Laboratory, University of Liverpool, Liverpool, United Kingdom⁵⁰Imperial College London, London, United Kingdom⁵¹School of Physics and Astronomy, University of Manchester, Manchester, United Kingdom⁵²Department of Physics, University of Oxford, Oxford, United Kingdom⁵³Syracuse University, Syracuse, New York, United States, USA⁵⁴Pontifícia Universidade Católica do Rio de Janeiro (PUC-Rio), Rio de Janeiro, Brazil, associated to Universidade Federal do Rio de Janeiro (UFRJ), Rio de Janeiro, Brazil⁵⁵Physikalisch Institut, Universität Rostock, Rostock, Germany, associated to Physikalisches Institut, Ruprecht-Karls-Universität Heidelberg, Heidelberg, Germany
(Received 19 March 2012; published 7 May 2012)

A study of $B^\pm \rightarrow J/\psi \pi^\pm$ and $B^\pm \rightarrow \psi(2S)\pi^\pm$ decays is performed with data corresponding to 0.37 fb^{-1} of proton-proton collisions at $\sqrt{s} = 7 \text{ TeV}$. Their branching fractions are found to be $\mathcal{B}(B^\pm \rightarrow J/\psi \pi^\pm) = (3.88 \pm 0.11 \pm 0.15) \times 10^{-5}$ and $\mathcal{B}(B^\pm \rightarrow \psi(2S)\pi^\pm) = (2.52 \pm 0.26 \pm 0.15) \times 10^{-5}$, where the first uncertainty is related to the statistical size of the sample and the second quantifies systematic effects. The measured CP asymmetries in these modes are $A_{CP}^{J/\psi\pi} = 0.005 \pm 0.027 \pm 0.011$ and $A_{CP}^{\psi(2S)\pi} = 0.048 \pm 0.090 \pm 0.011$ with no evidence of direct CP violation seen.

DOI: 10.1103/PhysRevD.85.091105

PACS numbers: 13.25.-k

^aP.N. Lebedev Physical Institute, Russian Academy of Science (LPI RAS), Moscow, Russia^bUniversità di Bari, Bari, Italy^cUniversità di Bologna, Bologna, Italy^dUniversità di Cagliari, Cagliari, Italy^eUniversità di Ferrara, Ferrara, Italy^fUniversità di Firenze, Firenze, Italy^gUniversità di Urbino, Urbino, Italy^hUniversità di Modena e Reggio Emilia, Modena, ItalyⁱUniversità di Genova, Genova, Italy^jUniversità di Milano Bicocca, Milano, Italy^kUniversità di Roma Tor Vergata, Roma, Italy^lUniversità di Roma La Sapienza, Roma, Italy^mUniversità della Basilicata, Potenza, ItalyⁿLIFAEELS, La Salle, Universitat Ramon Llull, Barcelona, Spain^oHanoi University of Science, Hanoi, Viet Nam

The Cabibbo-suppressed decay $B^+ \rightarrow \psi\pi^+$, where ψ represents either a J/ψ or $\psi(2S)$, proceeds via a $b \rightarrow c\bar{c}d$ quark transition. Its branching fraction is expected to be about 5% of the favored $b \rightarrow c\bar{s}$ mode, $B^+ \rightarrow \psi K^+$ (charge conjugation is implied unless otherwise stated). The standard model predicts that for $b \rightarrow c\bar{s}$ decays the tree and penguin contributions have the same weak phase and thus no direct CP violation is expected in $B^+ \rightarrow \psi K^+$. For $B^+ \rightarrow \psi\pi^+$, the tree and penguin contributions have different phases and CP asymmetries at the per mille level may occur [1]. An additional asymmetry may be generated, at the percent level, from long-distance rescattering, particularly from decays that have the same quark content ($D^0 D^-$, $D^{*-} D^0$, ...) [2]. Any asymmetry larger than this would be of significant interest.

In this paper, the CP asymmetries

$$A^{\psi\pi} = \frac{\mathcal{B}(B^- \rightarrow \psi\pi^-) - \mathcal{B}(B^+ \rightarrow \psi\pi^+)}{\mathcal{B}(B^- \rightarrow \psi\pi^-) + \mathcal{B}(B^+ \rightarrow \psi\pi^+)} \quad (1)$$

and charge-averaged ratios of branching fractions

$$R^\psi = \frac{\mathcal{B}(B^\pm \rightarrow \psi\pi^\pm)}{\mathcal{B}(B^\pm \rightarrow \psi K^\pm)} \quad (2)$$

are measured with the ψ reconstructed in the $\mu^+\mu^-$ final state. From the latter, $\mathcal{B}(B^\pm \rightarrow \psi\pi^\pm)$ may be deduced using the established $B^\pm \rightarrow \psi K^\pm$ branching fractions [3]. The CP asymmetry for $B^+ \rightarrow \psi(2S)K^+$ is also reported. $B^+ \rightarrow J/\psi K^+$ acts as a control mode in the asymmetry analysis because it is well measured and no CP violation is observed [3]. Previous measurements of the $B^+ \rightarrow J/\psi\pi^+$ branching fractions and CP asymmetries [4,5] have an accuracy of about 10%. The $B^+ \rightarrow \psi(2S)h^+(h = K, \pi)$ system is less precisely known due to a factor ten lower branching fraction to the $h\mu\mu$ final state. The world average for $A^{\psi(2S)K}$ is -0.025 ± 0.024 [3] and there has been one measurement of $A^{\psi(2S)\pi} = 0.022 \pm 0.086$ [6].

The LHCb experiment [7] takes advantage of the high $b\bar{b}$ and $c\bar{c}$ cross sections at the Large Hadron Collider to record unprecedented samples of heavy hadron decays. It instruments the pseudorapidity range $2 < \eta < 5$ of the proton-proton (pp) collisions with a dipole magnet and a tracking system which achieves a momentum resolution of 0.4–0.6% in the range 5–100 GeV/ c . The dipole magnet can be operated in either polarity and this feature is used to reduce systematic effects due to detector asymmetries. In the sample analyzed here, 55% of data was taken with one polarity, 45% with the other.

The pp collisions take place inside a silicon-strip vertex detector which has active material 8 mm from the beam line. It provides measurements of track impact parameters with respect to primary collision vertices (PV) and precise reconstruction of secondary B^+ vertices. Downstream muon stations identify muons by their penetration through layers of iron shielding. Charged particle identification (PID) is realized using ring-imaging Cherenkov detectors

with three radiators: aerogel, C_4F_{10} and CF_4 . Events with a high transverse energy cluster in calorimeters or a high transverse momentum (p_T) muon activate a hardware trigger. About 1 MHz of such events are passed to a software-implemented high level trigger, which retains about 3 kHz.

The analysis is performed using 0.37 fb^{-1} of data recorded by LHCb in the first half of 2011. The decay chain $B^+ \rightarrow \psi h^+$, $\psi \rightarrow \mu^+\mu^-$ is reconstructed from good quality tracks which have a track-fit χ^2 per degree of freedom < 5 . The muons are required to have momentum, $p > 3 \text{ GeV}/c$, and $p_T > 0.5 \text{ GeV}/c$. Selected hadrons have $p > 5 \text{ GeV}/c$ and $p_T > 1 \text{ GeV}/c$. The two muon candidates are used to form a ψ resonance with vertex-fit $\chi^2 < 10$. The dimuon invariant mass is required to be within $^{+30}_{-40} \text{ MeV}/c^2$ of the nominal ψ mass [3]; the asymmetric limits allow for a radiative tail.

The reconstructed B^+ candidate vertex is required to be of good quality with a vertex-fit $\chi^2 < 10$. It is ensured to originate from a PV by requiring $\chi_{\text{IP}}^2 < 25$ where the χ^2 considers the uncertainty on track impact parameters and the PV position. In addition, the angle between the B^+ momentum vector and its direction of flight from the PV must be $< 32(10) \text{ mrad}$ for $\psi(2S)h^+$ ($J/\psi h^+$). Furthermore, neither the muons nor the hadron track may point back to any primary vertex with $\chi_{\text{IP}}^2 < 4$. It is required that the hardware trigger accepted a muon from the B^+ candidate or by activity in the rest of the event. Hardware-trigger decisions based on the hadron are neglected to remove dependence on the correct emulation of the calorimeter's response to pions and kaons.

The B^+ candidates are refitted [8] requiring all three tracks to originate from the same point in space and the ψ candidates to have their nominal mass [3]. Candidates for which one muon gives rise to two tracks in the reconstruction, one of which is then assumed to be the hadron, form an artificial peaking background in the $\psi(2S)h^+$ analysis. These candidates peak in the invariant mass distribution of the same-sign muon-pion combination at $m_{\mu\pi} \sim 245 \text{ MeV}/c^2$, i.e. the sum of the muon and pion rest masses. Requiring $m_{\mu\pi} > 300 \text{ MeV}/c^2$ removes this background. In 2% of events two B^+ candidates are found. If they decay within 2 mm of each other the candidate with the poorest quality vertex is removed; otherwise both are kept.

When selecting $J/\psi h^+$ candidates, a requirement is made on the decay angle of the charged hadron as measured in the rest frame of the B^+ with respect to the B^+ trajectory in the laboratory frame, $\cos(\theta_h^*) < 0$. This requires the hadron to have flown counter to the trajectory of the B^+ candidate, hence lowering its average momentum in the laboratory frame. At lower momentum, the pion-kaon mass difference provides sufficient separation in the B^+ invariant mass distribution, as shown in Fig. 1. In the $B^+ \rightarrow \psi(2S)h^+$ analysis, the average momentum of the hadrons is lower, so such a cut is unnecessary to separate the two modes.

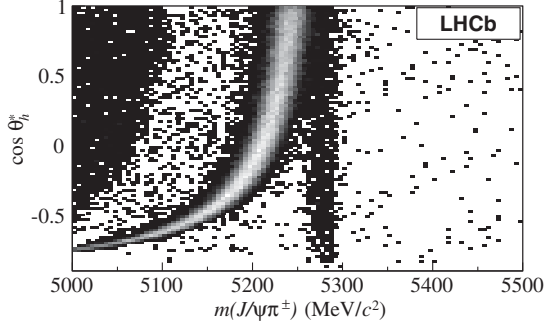


FIG. 1. Distribution of $\cos(\theta_h^*)$ versus the invariant mass of $B^+ \rightarrow J/\psi \pi^+$ candidates. The curved structure contains misidentified $B^+ \rightarrow J/\psi K^+$ decays which separate from the $B^+ \rightarrow J/\psi \pi^+$ vertical band for $\cos(\theta_h^*) < 0$. The partially reconstructed background, $B \rightarrow J/\psi K\pi$ enters top left.

Particle identification information is quantified as differences between the logarithm of likelihoods, $\ln \mathcal{L}_h$, under five mass hypotheses, $h \in \{\pi, K, p, e, \mu\}$. Separation of $\psi \pi^+$ candidates from ψK^+ is ensured by requiring that the hadron track satisfies $\ln \mathcal{L}_K - \ln \mathcal{L}_\pi = \text{DLL}_{K\pi} < 6$. This value is chosen to ensure that most ($\sim 95\%$) $B^+ \rightarrow \psi \pi^+$ decays are reconstructed as such. These events form the “pionlike” sample, as opposed to the kaonlike events satisfying $\text{DLL}_{K\pi} > 6$ that are reconstructed under the ψK^+ hypothesis.

The selected data are partitioned by magnet polarity, charge and $\text{DLL}_{K\pi}$ of the hadron track. By keeping the two magnet polarity samples separate, residual detection

asymmetries between the left and right sides of the detector can be evaluated and hence factor out. Event yields are extracted by performing an unbinned, maximum-likelihood fit simultaneously to the eight distributions of B invariant mass in the range $5000 < m_B < 5780$ MeV/ c^2 [9]. Figure 2 shows this fit to the data for $B^+ \rightarrow J/\psi h^+$, summed over magnet polarity. The $B^+ \rightarrow \psi(2S)h^+$ data is shown in Fig. 3.

The probability density function (PDF) used to describe these distributions has several components. The correctly reconstructed, $B^+ \rightarrow \psi h^+$ events are modeled by the function,

$$f(x) \propto \exp\left(\frac{-(x - \mu)^2}{2\sigma^2 + (x - \mu)^2\alpha_{L,R}}\right), \quad (3)$$

which describes an asymmetric peak of mean μ and width σ , and where $\alpha_L(x < \mu)$ and $\alpha_R(x > \mu)$ parameterize the tails. The mean is required to be the same for ψK^+ and $\psi \pi^+$ though it can vary across the four charge \times polarity subsamples to account for different misalignment effects. Table I shows the fitted values of the common tail parameters and the widths of the $B^+ \rightarrow \psi h^+$ peaks averaged over the subsamples.

The misidentified ψK^+ events form a displaced peaking structure to the left of the $\psi \pi^+$ signal and tapers to lower mass. This is modeled by a Crystal Ball function [10] which is found to be a suitable effective PDF. Its yield is added to that of the correctly identified events to calculate the total number of ψK^+ events.

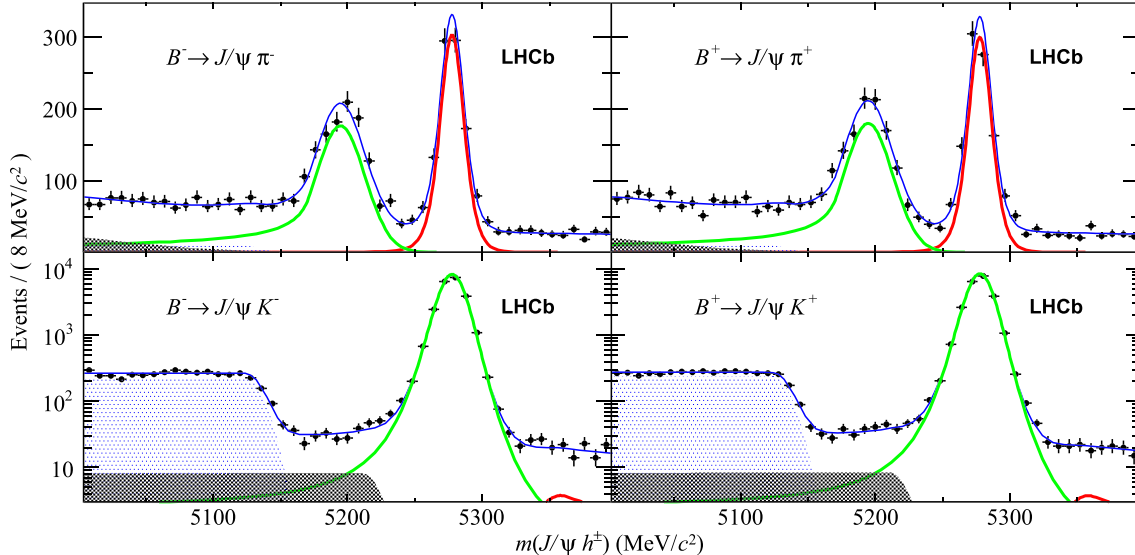


FIG. 2 (color online). Distributions of $B^\pm \rightarrow J/\psi h^\pm$ invariant mass, overlaid by the total fitted PDF (thin line). Pion-like events, with $\text{DLL}_{K\pi} < 6$ are reconstructed as $J/\psi \pi^\pm$ and enter in the top plots. All other events are reconstructed as $J/\psi K^\pm$ and are shown in the bottom plots on a logarithmic scale. B^- decays are shown on the left, B^+ on the right. The dark [red] curve shows the $B^\pm \rightarrow J/\psi \pi^\pm$ component, the light [green] curve represents $B^\pm \rightarrow J/\psi K^\pm$. The partially reconstructed contributions are shaded. In the lower plots these are visualized with a dark (light) shade for B^0 's (B^+ or B^0) decays. In the top plots the shaded component are contributions from $B \rightarrow J/\psi K^\pm \pi$ (dark) and $B \rightarrow J/\psi \pi^\pm \pi$ (light).

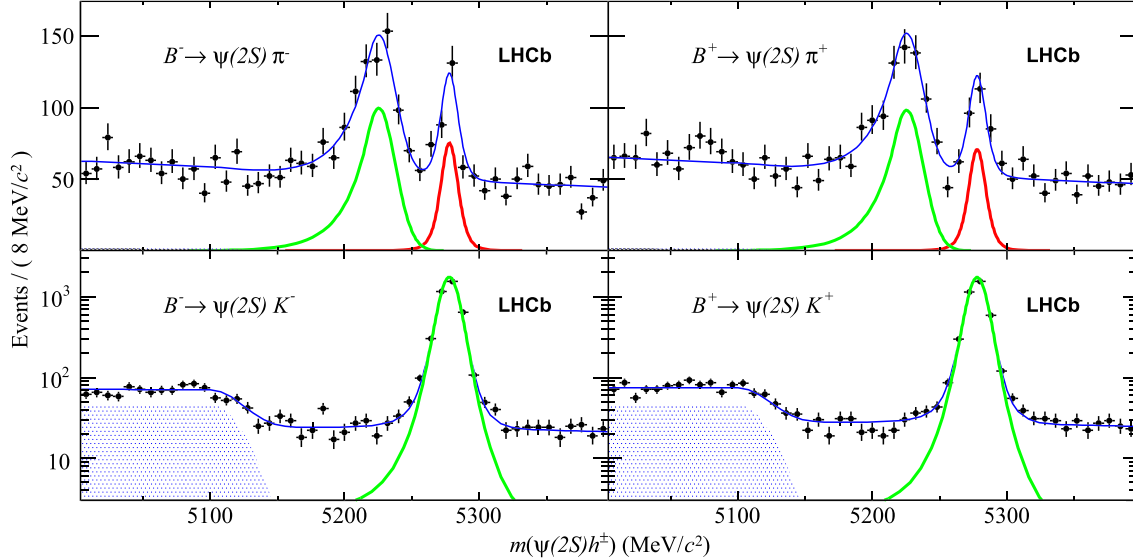


FIG. 3 (color online). Distributions of $B^\pm \rightarrow \psi(2S)h^\pm$ invariant mass. See the caption of Fig. 2 for details. The partially reconstructed background in the pionlike sample is present but negligible yields are found.

The PDF modelling the small component of $\psi\pi^+$ decays with $DLL_{K\pi} > 6$ is fixed entirely from simulation. It contributes negligibly to the total likelihood so the yield must be fixed with respect to that of correctly identified $\psi\pi^+$ events. The efficiency of the PID cut is estimated using samples of pions and kaons from $D^0 \rightarrow K^+\pi^-$ decays which are selected with high purity without using PID information. These calibration events are reweighted in bins of momentum to match the momentum distribution of the large $J/\psi K^+$ and $\psi(2S)K^+$ samples. By this technique, the following efficiencies are deduced for $DLL_{K\pi} < 6$: $\epsilon_{J/\psi\pi} = (95.8 \pm 1.0)\%$; $\epsilon_{\psi(2S)\pi} = (96.6 \pm 1.0)\%$. The errors, estimated from simulation, account for imperfections in the reweighting and the difference of the signal K^+ and π^+ momenta.

Partially reconstructed decays populate the region below the B^+ mass. $B^{+/0} \rightarrow \psi K^+\pi$ decays, where the pion is missed, are modeled in the kaonlike sample by a flat PDF with a Gaussian edge. A small $\bar{B}_s^0 \rightarrow \psi K^+\pi^-$ component is needed to achieve a stable fit. It is modeled with the same shape as the partially reconstructed $B^{+/0}$ decays except shifted in mass by the $B_s^0 - B^0$ mass difference, $+87 \text{ MeV}/c^2$. In the pionlike sample, $\psi\pi^+\pi^-$ backgrounds are assumed to enter with the same PDF, and same proportion relative to the signal, as the $\psi K^+\pi^-$ back-

ground in the kaonlike sample. A component of misidentified $B^{+/0} \rightarrow J/\psi K^+\pi$ is also included with a fixed shape estimated from the data. Lastly, a linear polynomial with a negative gradient is used to approximate the combinatorial background. The slope of this component of the pionlike and kaonlike backgrounds can differ.

The stability of the fit is tested with a large sample of pseudoexperiments. Pull distributions from these tests are consistent with being normally distributed, demonstrating that the fit is stable under statistical variations. The yields obtained from the signal extraction fit are shown in Table II.

The observables, defined in Eqs. (3) and (4) are calculated by the fit, then modified by a set of corrections taken from simulation. The acceptances of $\psi\pi^+$ and ψK^+ events in the detector are computed using PYTHIA [11] to generate the primary collision and EVTGEN [12] to model the B^+ decay. The efficiency of reconstructing and selecting $\psi\pi^+$ and ψK^+ decays is estimated with a bespoke simulation of LHCb based on GEANT4 [13]. It models the

TABLE II. Raw fitted yields. The labels ‘‘D’’ and ‘‘U’’ refer to the two polarities of the LHCb dipole.

			B^-	B^+
J/ψ	π	D	528 ± 27	518 ± 27
	π	U	421 ± 23	428 ± 23
	K	D	$13\,363 \pm 180$	$13\,466 \pm 181$
	K	U	$10\,666 \pm 148$	$11\,120 \pm 155$
$\psi(2S)$	π	D	94 ± 16	93 ± 16
	π	U	82 ± 15	70 ± 13
	K	D	2331 ± 88	2463 ± 93
	K	U	2026 ± 78	1836 ± 71

TABLE I. Signal shape parameters from the $B^\pm \rightarrow \psi h^\pm$ fits.

	J/ψ	$\psi(2S)$
$\sigma_{\psi K}$ (MeV/c^2)	7.84 ± 0.04	6.02 ± 0.08
$\sigma_{\psi\pi}$ (MeV/c^2)	8.58 ± 0.27	6.12 ± 0.75
α_L	0.12 ± 0.03	0.14 ± 0.01
α_R	0.10 ± 0.03	0.13 ± 0.01

TABLE III. Summary of systematic uncertainties. The statistical fit errors are included for comparison.

	$R^{J/\psi} (\times 10^{-2})$	$A^{J/\psi\pi}$	$R^{\psi(2S)} (\times 10^{-2})$	$A^{\psi(2S)\pi}$	$A^{\psi(2S)K}$
Simulation uncertainty	0.045	...	0.088
PID efficiencies	0.043	...	0.052
$A^{J/\psi K}$ (PDG [3])	...	0.0070	...	0.0070	0.0070
$A_{\text{Raw}}^{J/\psi K}$ statistical error	...	0.0046	...	0.0046	0.0046
Detection asymmetries	...	0.0056	...	0.0056	...
Relative trigger efficiency	0.020	0.0031	0.050	0.0036	0.0003
Fixed fit parameters	0.005	0.0006	0.017	0.0013	0.0001
Sum in quadrature (syst.)	0.065	0.0106	0.115	0.0108	0.0084
Fit error (stat.)	0.110	0.0268	0.404	0.0901	0.0136

interaction of muons and the two hadron species with the detector material. The total correction $\epsilon^{\psi K}/\epsilon^{\psi\pi}$ is 0.985 ± 0.012 and 1.007 ± 0.021 for $R^{J/\psi}$ and $R^{\psi(2S)}$ respectively.

CP asymmetries are extracted from the observed charge asymmetries (A_{Raw}) by taking account of instrumentation effects. The interaction asymmetry of kaons, A_{Det}^K , is expected to be nonzero, especially for low-momentum particles. This asymmetry, measured at LHCb using a sample of $D^{*+} \rightarrow D^0\pi^+$, $D^0 \rightarrow K^+\pi^-$ decays, is -0.010 ± 0.002 if the pion asymmetry is zero [14]. The null-asymmetry assumption for pions has been verified at LHCb to an accuracy of 0.25% [15]. These results are used with enlarged uncertainties (0.004, for both kaons and pions) to account for the different momentum spectra of this sample and those used in the previous analyses.

In summary, the CP asymmetry is defined as

$$A^{\psi h} = A_{\text{Raw}}^{\psi h} - A_{\text{Prod}} - A_{\text{Det}}^h, \quad (4)$$

where the production asymmetry, A_{Prod} , describes the different rates with which B^- and B^+ hadronize out of the pp collisions. The observed, raw charge asymmetry in $B^+ \rightarrow J/\psi K^+$ is -0.012 ± 0.004 . Using Eq. (4) with the established CP asymmetry, $A^{J/\psi K} = 0.001 \pm 0.007$ [3], A_{Prod} is estimated to be -0.003 ± 0.009 . This is applied as a correction to the other modes reported here.

The different contributions to the systematic uncertainties are summarized in Table III. They are assessed by modifying the final selection, or altering fixed parameters and rerunning the signal yield fit. The maximum variation of each observable is taken as their systematic uncertainty.

The largest uncertainty is due to the use of simulation to estimate the acceptance and selection efficiencies. It accounts for any bias due to imperfect modelling of the detector and its relative response to pions and kaons. Another important contribution arises from the loose trigger criteria that are employed. This uncertainty is estimated from the shift in the central values after rerunning the fit using only those events where the muons passed the software trigger. The use of the PID calibration to estimate the efficiency for pions to the $\text{DLL}_{K\pi} < 6$ selection also contributes a significant systematic uncertainty.

The measurements of $A^{\psi\pi}$ depend on the estimation of A_{Prod} from the $B^+ \rightarrow J/\psi K^+$ channel. The uncertainty on A_{Prod} is determined by the statistical error of $A_{\text{Raw}}^{J/\psi K}$ in the fit, the uncertainty on the world average of $A^{J/\psi K}$ and the estimation of A_{Det}^h . These effects are kept separate in the table where it is seen that the uncertainty on the nominal value of $A^{J/\psi K}$ dominates. Finally, it is noted that the detector asymmetries cancel for $A^{\psi(2S)K}$ and a lower systematic uncertainty can be reported.

The measured ratios of branching fractions are

$$\begin{aligned} R^{J/\psi} &= (3.83 \pm 0.11 \pm 0.07) \times 10^{-2} \\ R^{\psi(2S)} &= (3.95 \pm 0.40 \pm 0.12) \times 10^{-2}, \end{aligned}$$

where the first uncertainty is statistical and the second systematic. $R^{\psi(2S)}$ is compatible with the one existing measurement, $(3.99 \pm 0.36 \pm 0.17) \times 10^{-2}$ [6]. The measurement of $R^{J/\psi}$ is 3.2σ lower than the current world average, $(5.2 \pm 0.4) \times 10^{-2}$ [3]. Using the established measurements of the Cabibbo-favored branching fractions [3], we deduce

$$\begin{aligned} \mathcal{B}(B^\pm \rightarrow J/\psi \pi^\pm) &= (3.88 \pm 0.11 \pm 0.15) \times 10^{-5} \\ \mathcal{B}(B^\pm \rightarrow \psi(2S)\pi^\pm) &= (2.52 \pm 0.26 \pm 0.15) \times 10^{-5}, \end{aligned}$$

where the systematic uncertainties are summed in quadrature. The measured CP asymmetries,

$$\begin{aligned} A_{CP}^{J/\psi\pi} &= 0.005 \pm 0.027 \pm 0.011 \\ A_{CP}^{\psi(2S)\pi} &= 0.048 \pm 0.090 \pm 0.011 \\ A_{CP}^{\psi(2S)K} &= 0.024 \pm 0.014 \pm 0.008, \end{aligned}$$

have comparable or better precision than previous results, and no evidence of direct CP violation is seen.

We express our gratitude to our colleagues in the CERN accelerator departments for the excellent performance of the LHC. We thank the technical and administrative staff at CERN and at the LHCb institutes, and acknowledge support from the National Agencies: CAPES, CNPq, FAPERJ and FINEP (Brazil); CERN; NSFC (China); CNRS/IN2P3 (France); BMBF, DFG, HGF and MPG (Germany); SFI

R. AAIJ *et al.*

(Ireland); INFN (Italy); FOM and NWO (The Netherlands); SCSR (Poland); ANCS (Romania); MinES of Russia and Rosatom (Russia); MICINN, XuntaGal and GENCAT (Spain); SNSF and SER (Switzerland);

PHYSICAL REVIEW D **85**, 091105(R) (2012)

NAS Ukraine (Ukraine); STFC (United Kingdom); NSF (USA). We also acknowledge the support received from the ERC under FP7 and the Region Auvergne.

-
- [1] I. Dunietz and J.M. Soares, *Phys. Rev. D* **49**, 5904 (1994).
 - [2] J.M. Soares, *Phys. Rev. D* **52**, 242 (1995).
 - [3] K. Nakamura *et al.* (Particle Data Group), *J. Phys. G* **37**, 075021 (2010).
 - [4] B. Aubert *et al.* (*BABAR* Collaboration), *Phys. Rev. Lett.* **92**, 241802 (2004).
 - [5] V. Abazov *et al.* (*D0* Collaboration), *Phys. Rev. Lett.* **100**, 211802 (2008).
 - [6] V. Bhardwaj *et al.* (*Belle* Collaboration), *Phys. Rev. D* **78**, 051104 (2008).
 - [7] A. A. Alves, Jr. *et al.* (*LHCb* Collaboration), *JINST* **3**, S08005 (2008).
 - [8] W.D. Hulsbergen, *Nucl. Instrum. Methods Phys. Res., Sect. A* **552**, 566 (2005).
 - [9] W. Verkerke and D. Kirkby, in *2003 Computing in High Energy and Nuclear Physics (CHEP03), La Jolla, CA, USA, March 2003*, eConf C0303241, MOLT007 (2003), [arXiv:physics/0306116](https://arxiv.org/abs/physics/0306116).
 - [10] T. Skwarnicki, PhD thesis, Institute of Nuclear Physics, Krakow, 1986, Report No. DESY-F31-86-02.
 - [11] T. Sjöstrand, S. Mrenna, and P. Skands, *J. High Energy Phys.* **05** (2006) 026.
 - [12] D.J. Lange, *Nucl. Instrum. Methods Phys. Res., Sect. A* **462**, 152 (2001).
 - [13] S. Agostinelli *et al.* (*GEANT4* Collaboration), *Nucl. Instrum. Methods Phys. Res., Sect. A* **506**, 250 (2003).
 - [14] R. Aaij *et al.* (*LHCb* Collaboration), [arXiv:1202.6251](https://arxiv.org/abs/1202.6251).
 - [15] R. Aaij *et al.* (*LHCb* Collaboration LHCb-PAPER-2012-009.